Electrical Conductance Tuning and Bistable Switching in Poly(*N*-vinylcarbazole)−Carbon Nanotube Composite Films

Gang Liu,[†] Qi-Dan Ling,[†] Eric Yeow Hwee Teo,[‡] Chun-Xiang Zhu,[‡] D. Siu-Hung Chan,[‡] Koon-Gee Neoh,[†] and En-Tang Kang[†,*]

[†]Department of Chemical & Biomolecular Engineering and [‡]Department of Electrical & Computer Engineering, National University of Singapore, Kent Ridge, Singapore 119260

ABSTRACT By varying the carbon nanotube (CNT) content in poly(*N*-vinylcarbazole) (PVK) composite thin films, the electrical conductance behavior of an indium−tin oxide/PVK−CNT/aluminum (ITO/PVK−CNT/Al) sandwich structure can be tuned in a controlled manner. Distinctly different electrical conductance behaviors, such as (i) insulator behavior, (ii) bistable electrical conductance switching effects (write-once read-many-times (WORM) memory effect and rewritable memory effect), and (iii) conductor behavior, are discernible from the current density−voltage characteristics of the composite films. The turn-on voltage of the two bistable conductance switching devices decreases and the ON/OFF state current ratio of the WORM device increases with the increase in CNT content of the composite film. Both the WORM and rewritable devices are stable under a constant voltage stress or a continuous pulse voltage stress, with an ON/OFF state current ratio in excess of 10^3. The conductance switching effects of the composite films have been attributed to electron trapping in the CNTs of the electron-donating/hole-transporting PVK matrix.

KEYWORDS: PVK · carbon nanotube · conductance switching · memory · WORM · rewritable · charge trapping

In recent years, polymeric materials and their composites with carbon nanotube (CNT) have found extensive applications in organic electronics.[1,2] Numerous molecular electronic devices, including light-emitting diodes,[3,4] photovoltaic cells,[5−7] transistors,[8] sensors,[9] and memories,[10−14] have been demonstrated. Polymer/organic electronic memories exhibit structural simplicity, good scalability, high mechanical flexibility, and low fabrication cost, making them a potential alternative or supplementary technology to the inorganic semiconductor information technology.[15,16] Rather than encoding "0" and "1" as the amount of charges stored in a cell, a polymer/organic memory stores data in a different manner, for example, based on the high and low conductivity response to an applied electric field.[17] In earlier works on polymer memory, a number of polymeric materials have been studied directly,[18] as well as have been used as polyelectrolytes,[19] as components of charge transfer complexes,[20] or as matrix of dyes in doped or mixed systems.[21−24] The materials, devices, and mechanism aspects of polymer electronic memories have been reviewed recently.[25]

In view of many interesting works on electrical switching and memory effects in doped or mixed polymer systems,[21−24] the effect of doping level on the electrical behavior of polymeric systems seemingly deserves further exploration. It is reasonable to expect that doping levels will significantly affect charge transport processes in the bulk and at the interface and consequently will have an important influence on device performance.[26] In this work, we report the controllable electrical conductance switching and nonvolatile memory effects in poly(*N*-vinyl carbazole) (PVK, shown in Figure 1) and carbon nanotube composite thin films. The electrical and bistable switching behaviors of the PVK−CNT composite films can be tuned by varying the CNT content (doping level) in the composite films. Unique device behaviors, including (i) insulator behavior, (ii) bistable electrical conductance switching effects (write-once read-many-times (WORM) memory and rewritable memory effects), and (iii) conductor behavior, can be realized in an ITO/PVK−CNT/Al sandwich structure by increasing the CNT content in the PVK−CNT composite film.

RESULTS AND DISCUSSION

The electrical properties and switching effects of the ITO/PVK−CNT/Al sandwich

*Address correspondence to cheket@nus.edu.sg.

Received for review March 31, 2009 and accepted May 25, 2009.

Published online June 1, 2009.
10.1021/nn900319q CCC: $40.75

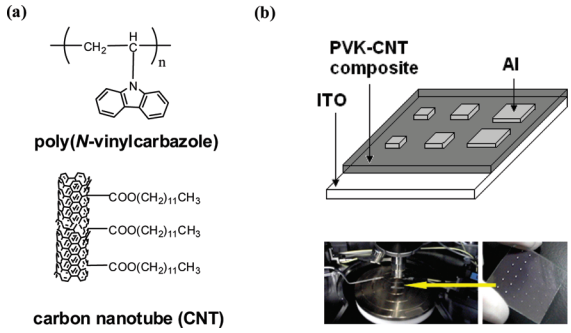

Figure 1. (a) Structural formulas of poly(*N*-vinylcarbazole) and surfaced-functionalized carbon nanotube, and (b) schematic diagram of the ITO/PVK−CNT/Al sandwich devices.

structures are illustrated by the current density−voltage (*J*−*V*) characteristics of Figure 2. Due to the insulating nature of pure PVK, the PVK film without any CNT content exhibits only a low conductivity (insulating) state. Doping the film with 0.2% CNT does not affect the device performance significantly (Figure 2a), except for an increase in electrical conductivity. The *J*−*V* characteristics of devices with 0.5 and 1% CNT contents are similar, and both display distinctly bistable electrical conductivity states. Starting with the low conductivity (OFF) state in the device containing 1% CNT content (Figure 2b), the current density increases gradually with the increase in applied negative voltage (Al as cathode). The current density remains low, until the threshold voltage (turn-on voltage) of about −2.2 V is reached. At the turn-on voltage, the current density increases abruptly from 10^{-4} to 1 A/cm^2 (Sweep 1), indicating device transition from the low conductivity (OFF) to the high conductivity (ON) state. In the subsequent negative sweep (Sweep 2), the device remains in its high conductivity state, with an ON/OFF state current ratio of about 10^4 when read at −1 V. The transition from the OFF state to the ON state serves as the "writing" process for the memory device, and "0" and "1" can be encoded from the low conductivity state and high conductivity state, respectively. After a reverse sweep to +4 V (Sweep 3), the high conductivity state is maintained, thereby suggesting the write-once read-many-times (WORM) memory behavior for the 1% CNT-containing device. The device containing 0.5% CNT switches at a slightly higher voltage of −2.5 V with a slightly lower ON/OFF state current ratio of about 2×10^3 and exhibits similar WORM memory switching behavior.

The device with 2% CNT content also exhibits bistable electrical switching behavior, as illustrated by the *J*−*V* characteristics of Figure 2c. With the increased CNT content in the composite film, both the OFF and ON state current densities have increased. The device exhibits a significantly lower turn-on voltage of −1.8 V and an ON/OFF state current ratio of 5×10^3 (Sweep 1). However, after reading the ON state in the negative sweep (Sweep 2), a positively biased sweep (Sweep 3) can program the ON state back to the original OFF state at 2.9 V. The positive voltage sweep thus serves as the "erase" process for the rewritable memory device. The OFF state of the device can be read (Sweep 4) and reprogrammed to the ON state again in the subsequent negative sweep (Sweep 5), thus completing the "write-read-erase-read-rewrite" cycle. The cycle can be repeated with fairly good accuracy (inset of Figure 2c). The present ITO/PVK−CNT/Al devices were characterized under ambient conditions. The absorption and adsorption of air and moisture might have affected the electrical properties of the polymer and the polymer/metal interface.[27] The electrical stress might also have an effect on the inherent electrical relaxation of the polymer and organic materials.[25] Thus, a minor shift or fluctuation in switching voltages might be expected. The nonvolatile and reprogrammable switching behavior of the device based on the PVK−2% CNT composite film is characteristic of that of a rewritable memory. Further increase in CNT content results in a significant increase in the conductivity of the composite film, and devices with ≥3% CNT content all exhibit a single state conductor behavior (Figure 2d).

The *J*−*V* characteristics of ITO/PVK−CNT/Cu devices exhibit similar bistable conductivity switching behaviors, albeit with higher turn-on voltages (Figure 3). The increase in the turn-on voltage is consistent with the increase in the work function of metal electrode (−4.7 eV for Cu *vs* −4.3 eV for Al),[28] which leads to a higher energy barrier for electron injection from the electrode into the PVK matrix. The energy difference between the work function of Cu and the lowest unoccupied molecular orbital (LUMO) of PVK is 2.7 eV. However, the charge carrier injection barrier height at metal/PVK interface is still lower than the trap depth associated with the CNT/PVK interface (3.1 eV, or the energy difference between the work function of CNT, −5.1 eV, and the LUMO of PVK, −2.0 eV).[29−33] Regardless of whether the top metal electrode is Al or Cu, devices containing 1% CNT always exhibit WORM memory switching effect, while devices containing 2% CNT always exhibit rewritable memory switching effect. Thus, the conductance switching observed must be intrinsic to the PVK−CNT composite films. It has also been reported that the Al/polymer interface may play a role in the electrical bistability, and conductivity switching may occur in the native or electrically oxidized aluminum oxide layer.[34,35] However, the influence of any oxide layer on the switching phenomena observed in the present bistable conductivity switching devices can be ruled out by employing Cu or Au as the top electrode since Cu and Au are more inert and are less likely to be oxidized. Conductive metallic filaments may also form during thermal evaporation of the top electrode or upon application of an electric field to the sandwich device.[36−38] The resistance of the filaments should increase linearly with the increase in temperature, follow-

ing the behavior of a metallic conductor. Figure 3a,b shows the respective temperature-independent ON state currents of an ITO/PVK−CNT/Cu WORM memory device and an ITO/PVK−CNT/Cu rewritable memory device retrieved at −1 V. Both currents remain almost constant in the temperature range of 25−125 °C. Thus, the metallic filamentary conduction mechanism can be ruled out by the lack of an obvious temperature-dependent ON state current in the present devices. Moreover, it is unlikely that the filament formation is the origin of the conductance switching because the *J*−*V* characteristics of the PVK−CNT composite films are strongly dependent on the content of carbon nanotubes.

Carbazole moieties are well-known electron donors and hole transporters in organic electronics.[39,40] Carbazole-containing polymers can also form charge transfer (CT) complexes with appropriate electron acceptors. Memory devices based on PVK−2,4,7-trinitro-9-fluorenone (PVK−TNF) CT complexes have been demonstrated recently.[41] Pristine PVK film on ITO substrate exhibits optical absorption peaks at 290, 345, and 372 nm. By introducing CNT into the polymer film, the absorption peak of carbazole moieties at 372 nm is blue-shifted slightly, indicating the presence of weak localized interaction between the carbazole moieties of PVK and the carboxylic moieties of surfaced-functionalized CNTs. No significant change in line shape of the absorption spectrum is observed after switching the composite film containing 1% CNT to the ON state. The XPS C 1s and N 1s core-level spectra of the polymer composite film containing 1% CNT do not exhibit any significant change in binding energy or line shape after conductivity switching either. Thus, the observed conductivity switching is probably not induced by the CT interaction or complex formation between PVK and CNTs in the present composite films.

The *J*−*V* characteristics of the insulator, bistable devices, and conductor are fitted with appropriate charge transport models (Figure 4a−d). Due to low CNT content in the composite films, PVK is the dominant component and serves as the matrix of the active layer in the present devices. CNT has a much higher work function (−5.1 eV) compared to the LUMO level of PVK (−2.0 eV) and is more likely to serve as the electron trapping center and electron transporter.[29−33] Upon applying a negative voltage to the top (Al) electrode, electrons are injected into the composite film and trapped by the CNTs. The trapped electrons will induce a countering space-charge layer in PVK near the Al electrode. Under low bias, electrons do not have sufficient energy/mobility to escape from the isolated CNT trapping centers in the PVK matrix, and the small current is attributed to hole transport in the PVK matrix. The current of the insulator or the OFF state current of bistable devices can be fitted by a space-charge-limited current (SCLC) (Figure 4a)[42,43]

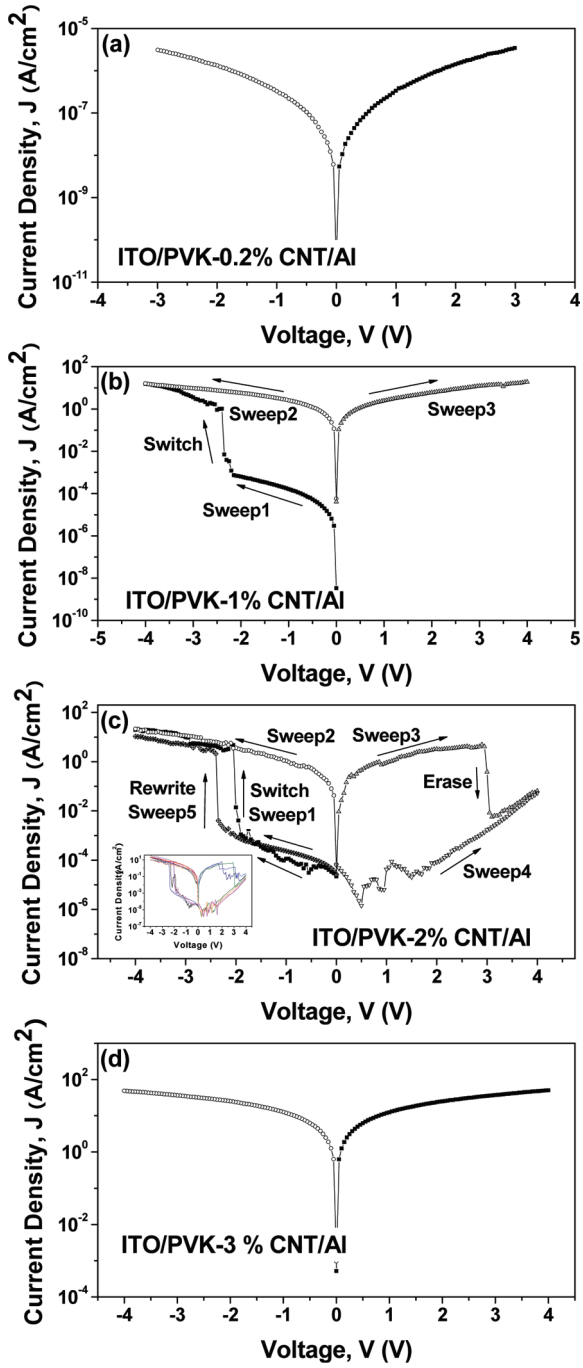

Figure 2. *J*−*V* characteristics of the ITO/PVK−CNT/Al devices containing (a) 0.2%, (b) 1%, (c) 2%, and (d) 3% carbon nanotubes.

$$J = A\frac{9}{8}\mu\varepsilon\varepsilon_0\frac{V^2}{d^3} \qquad (1)$$

where A is a positive constant, μ is the mobility of charge carriers, $\varepsilon\varepsilon_0$ is the absolute permittivity of the composite film, and d is the thickness of the composite film.

Charge carriers can acquire activation energy from an external electric field, and their mobility increases with the applied voltage sweeps.[42] In a 0.2% CNT-containing device, the large separation between nano-

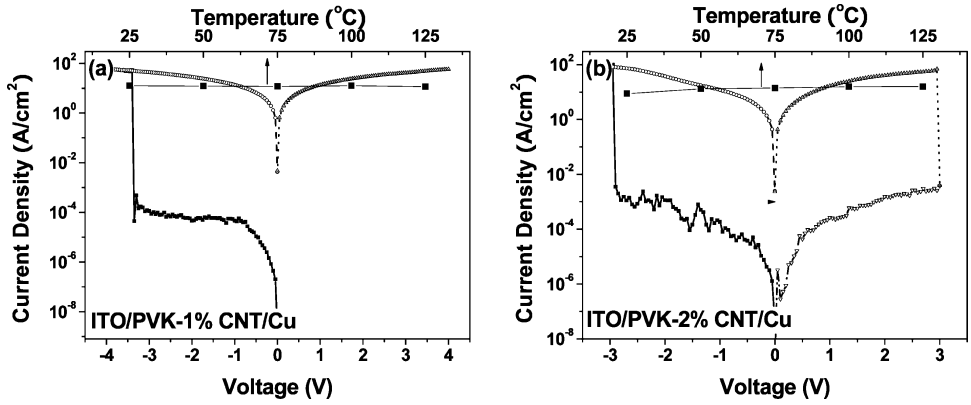

Figure 3. *J*−*V* characteristics of the ITO/PVK−CNT/Cu devices containing (a) 1% and (b) 2% carbon nanotubes.

tubes prevents the charge carriers from inter-nanotube hopping, resulting in a single low conductivity state. For devices containing 0.5−1% CNT, the distances between isolated nanotubes are reduced. At the threshold switching voltage, a majority of the charge trapping centers are filled, and a trap-free environment exists in the composite film. Percolation pathways for charge carriers among the CNTs are formed, allowing for inter-nanotube hopping and switching the devices from the low conductivity (OFF) state to the high conductivity (ON) state. The ON state currents of the WORM devices containing 0.5−1% CNT can be fitted by a space-charge (SC)-modulated Frenkel−Poole emission current (Figure 4b)[42]

$$J = A\frac{9}{8}\mu\varepsilon\varepsilon_0\frac{V^2}{d^3}\exp\left\{\frac{0.891}{kT}\left(\frac{q^3V}{\pi\varepsilon\varepsilon_0 d}\right)^{1/2}\right\} + BV\exp\left\{\frac{q}{kT}\left(\sqrt{\frac{qV}{\pi\varepsilon\varepsilon_0 d}} - \phi_B\right)\right\} \quad (2)$$

where k is the Boltzmann constant, T is the ambient temperature, q is the absolute value of the unit electronic charge (1.6×10^{-19} C), B is a positive constant, and φ_B is the energy barrier at the PVK−CNT interface (3.1 eV). With further increase in CNT concentration, the CNTs in the composite thin film can come into direct contact with both electrodes, eliminating the space-charge layer formed near the PVK−Al interface. The ON state current of the rewritable device containing 2% CNT can be fitted by a space-charge-free Frenkel−Poole emission current (Figure 4c)[42]

$$J = BV\exp\left\{\frac{q}{kT}\left(\sqrt{\frac{qV}{\pi\varepsilon\varepsilon_0 d}} - \phi_B\right)\right\} \quad (3)$$

Due to the strong electron-withdrawing ability of CNT and the extensive π-conjugation along the CNT axis, electrons are deeply trapped in the CNT network and stabilized by the PVK matrix (electron donor and hole transporter) throughout the entire composite film.[44] Thus, even after turning off the power supply, the CNT system still retains the trapped charge carriers and the charged state. Consequently, the composite film remains in the high conductivity (trap-filled) state, leading to the nonvolatile nature of the bistable device. When a reverse (positive) bias is applied to devices containing 0.5−1% CNT, the applied electric field is opposed by the build-in electric field associated with the space-charge layer in PVK. The build-in electric field will prevent the trapped electrons from being neutralized or extracted, and the devices remain in the high conductivity state, characteristic of the behavior of a WORM memory. For the device containing 2% CNT, the CNTs can come into contact with the electrode. The energy difference between the work function of CNT (−5.1 eV) and the work function of Al (−4.3 eV), as well as the donor nature of the PVK matrix, will prevent the trapped charges in CNTs from being detrapped when the power supply is turned off, leading to the nonvolatile nature of the memory device. Upon application of a reverse (positive) bias of sufficient magnitude and with the elimination of the space-charge layer in PVK near the polymer−electrode interface (when the CNTs come into contact with the electrodes), the trapped charges in the CNTs will be neutralized or extracted. As a result, the device returns to the original low conductivity state, characteristic of the behavior of a rewritable memory.

For devices containing ≥3% CNT, continuous π-conjugated networks are formed in the bulk films arising from the close stacking of the carbon nanotubes. This continuous network allows effective transport of charge carriers even under low bias, making the devices highly conductive. The single high conductivity state in devices containing 3% or more of CNT can be fitted by the Ohmic current (Figure 4d).

As shown in the FE-SEM images of Figure 5, carbon nanotubes are distributed uniformly in the PVK matrix. CNTs are well integrated into the polymer matrix, and it is difficult to distinguish individual CNT from the PVK matrix. The effect of CNT content in the composite films on device performance, including current density, turn-on voltage, and ON/OFF state current ratio, is summarized in Figure 6. The electrical conductivity of the composite films is enhanced by 6 orders of magnitude with the increase in CNT content from 0 to 3%. The turn-on voltage of the bistable devices decreases from −2.5 to −1.8 V, as the CNT content is increased from 0.5 to 2%. The decrease in the distance between isolated nanotubes leads to a lower activation energy (percolation threshold) for effective charge carrier hopping and thus a reduced threshold switching voltage. As a one-

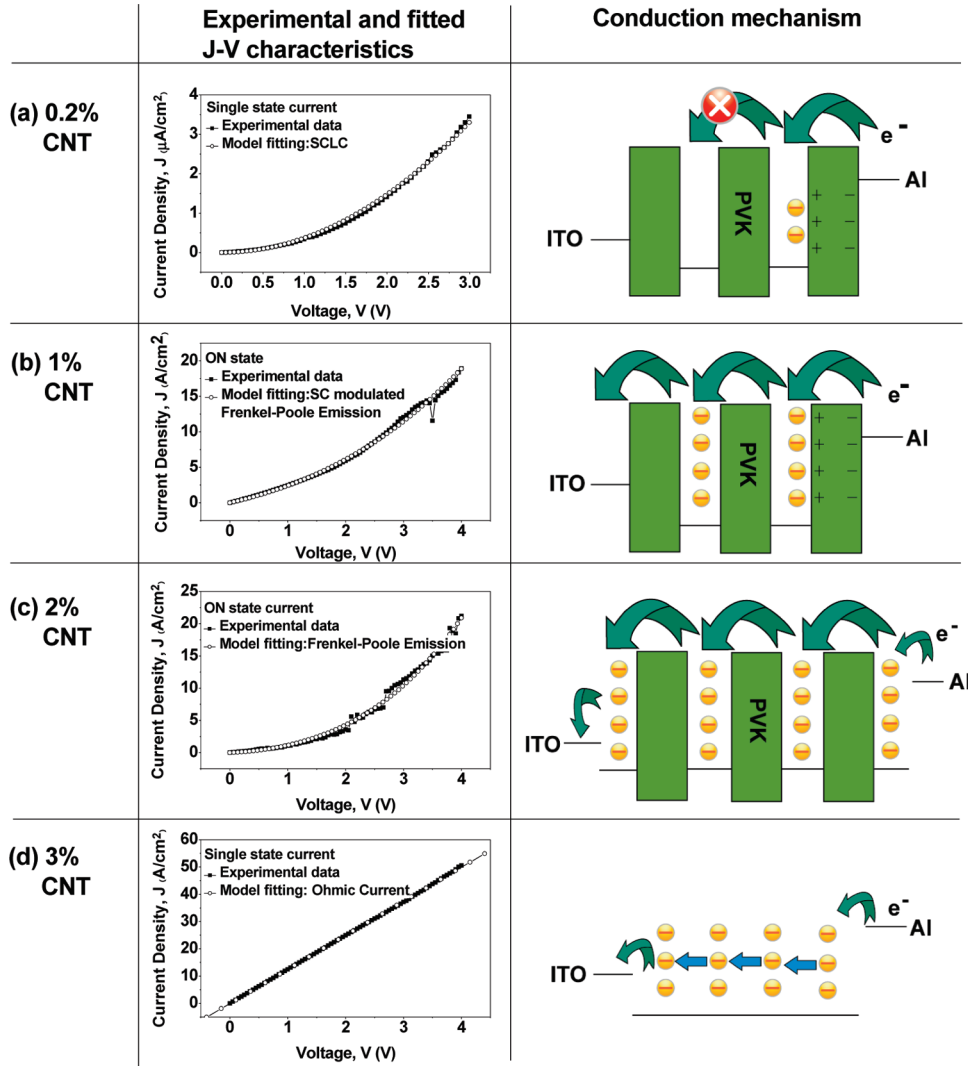

Figure 4. Experimental and fitted *J*−*V* characteristics, and conduction mechanism of the ITO/PVK−CNT/Al devices containing (a) 0.2%, (b) 1% (ON state), (c) 2% (ON state), and (d) 3% carbon nanotubes.

dimensional conductor along its axis, the orientation and alignment of CNTs are expected to have a significant effect on the electrical behavior of the composite films. Spin-casting of the composites on ITO substrates leads to a thin composite film with planar and random orientation of CNTs in the film. Thus, the device behavior associated with charge carrier trapping and inter-CNT hopping will be directly dependent on the effective distance between neighboring CNTs or the CNT content in the composite film. With CNT content increased from 0.2 to 3%, the distance between isolated nanotubes is significantly reduced from 150 to 10 nm (Table 1 and Supporting Information). A distance of 150 nm is too large for charge hopping in the PVK−0.2% CNT composite, compared to the diameter of individual carbon nanotube (15 nm). On the other hand, the effective distances of 30 nm (PVK−1% CNT composite) and 15 nm (PVK−2% CNT composite) are comparable to the diameter of individual carbon nanotube and are suitable for charge hopping among individual nanotubes. Finally, at the effective distance of 10 nm (PVK−3% CNT composite), which is even smaller than the diameter of individual carbon nanotubes, continuous electron pathways probably have formed. Due to the strong electron-withdrawing ability of CNT, a large number of electrons are captured by the CNTs in the WORM device. The higher CNT content also provides a larger number of electron pathways throughout the entire composite film. Once the threshold voltage is reached, a larger number of electrons are transferred *via* the increased number of carrier pathways, resulting in a significant increase in the ON state current and a consequent in-

TABLE 1. Effective Distance between Neighboring CNTs in the PVK-CNT Composite Films and the Corresponding Device Behavior (Diameter of CNT = 15 nm)

CNT content (weight percentage)	effective distance (nm)	device type
0.2%	150	insulator
1%	30	WORM memory
2%	15	rewritable memory
3%	10	conductor

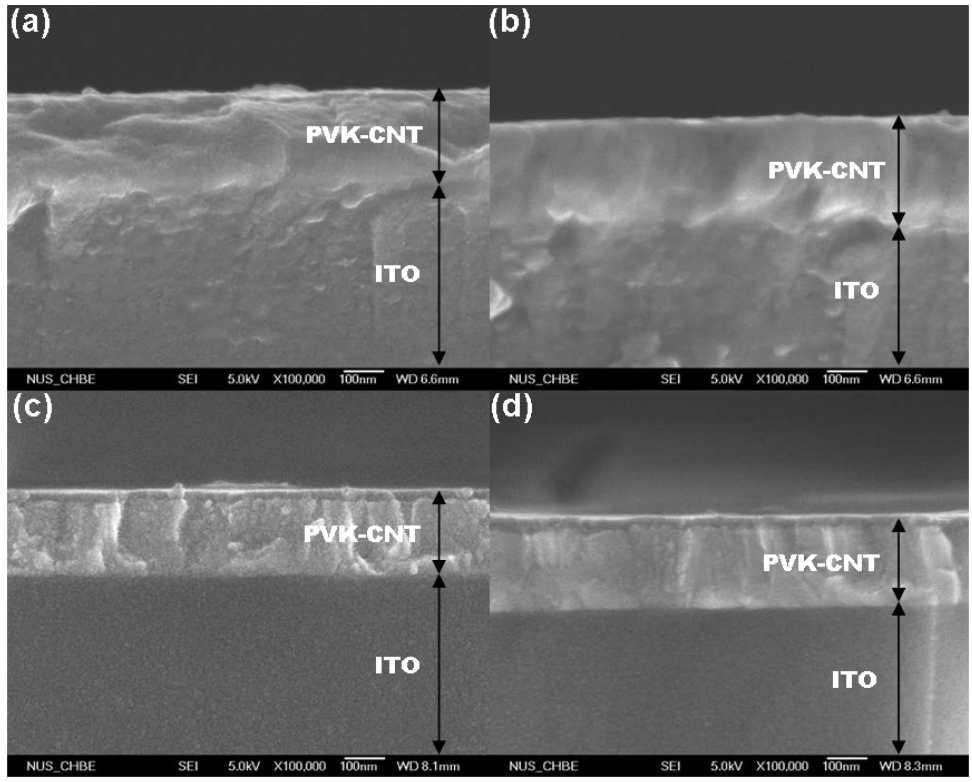

Figure 5. FE-SEM images (cross-sectional view) of the PVK−CNT composite films containing (a) 0.2%, (b) 1%, (c) 2%, and (d) 3% carbon nanotubes.

crease in the ON/OFF state current ratio. With the further increase in CNT content to 2% and the simultaneous decrease in distance between isolated nanotubes, charge carrier transport along the electron pathways *via* inter-CNT hopping becomes easier and occurs earlier than that in the WORM device, resulting in less charge carriers being trapped before switching. Thus, a smaller ON/OFF state current ratio is observed in the rewritable device.

Besides the large ON/OFF state current ratio, which promises a low misreading rate of the device during operation, stability against constant and pulse voltage stresses, as well as the switching time, are also important parameters in switching performance. The OFF and ON state currents in both the WORM and rewritable devices can be sustained under a constant voltage stress of −1 V for up to 3 h, as shown in Figure 7a,b, respectively. The ON and OFF states of both the WORM memory device (Figure 7c) and rewritable memory device (Figure 7d) are stable for up to 10^8 continuous read pulses of −1 V (pulse period = 2 μs, pulse width = 1 μs). The Al/PVK−CNT/ITO bistable devices have a switching time of ~10 μs (Supporting Information, Figure S3), which is slower than the writing time (1 to 0.1 μs) of the commercial silicon-based memory devices.[25] Upon proper encapsulation of the ITO/PVK−CNT/Al structure, the device performance is expected to improve.

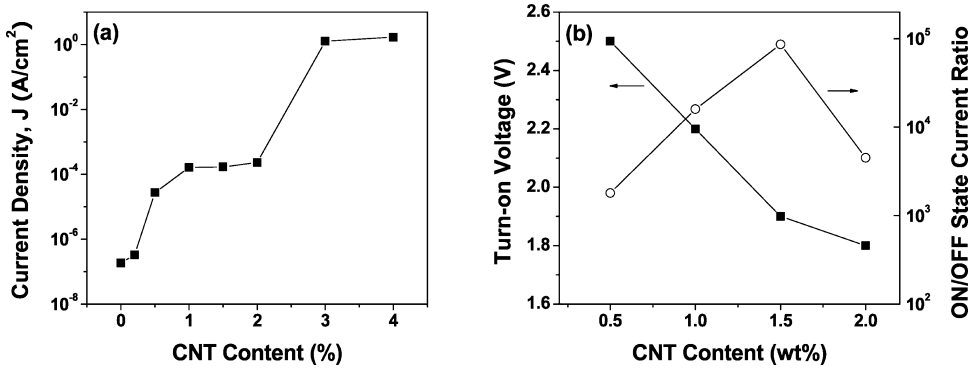

Figure 6. Effect of the carbon nanotube (CNT) content on the (a) current density [single-state (for the insulator and conductor devices) and OFF-state (for the electrical bistable devices) current densities when read at −1 V], and (b) turn-on voltage (absolute value) and ON/OFF state current ratio of the ITO/PVK−CNT/Al devices.

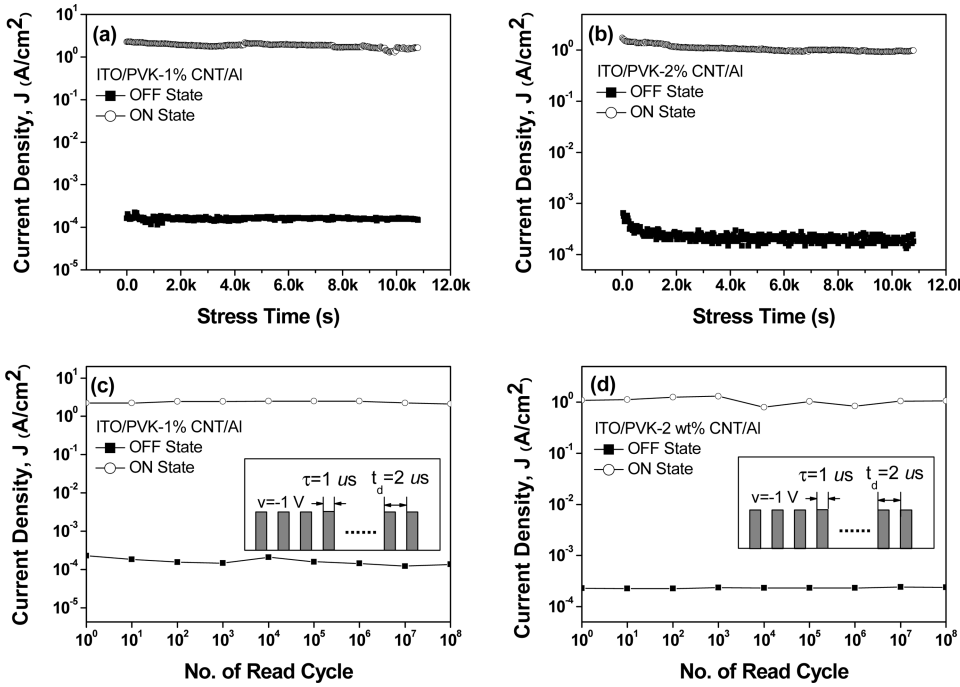

Figure 7. Stability of the ITO/PVK−CNT/Al devices containing 1 and 2% carbon nanotubes in the ON and OFF state, (a,b) under a constant stress of −1 V and (c,d) under a continuous read pulse with a peak voltage of −1 V, a pulse width of 1 μs, and a pulse period of 2 μs.

CONCLUSIONS

Through controlling the CNT content in the PVK−CNT composite film, electronic devices with a sandwich structure of ITO/PVK−CNT/Al are capable of exhibiting (i) insulator behavior, (ii) bistable electrical switching behavior (WORM memory and rewritable memory effects), and (iii) conductor behavior. In addition to different device behaviors, device performance parameters, including conductivity, turn-on voltage, and ON/OFF state current ratio, can also be tuned by varying the doping level, or the CNT content, in the composite films. The controllable electrical properties and nonvolatile electrical bistable switching effects in the composite films can be attributed to electron trapping in the carbon nanotubes of the electron-donating/hole-transporting PVK matrix.

MATERIALS AND METHODS

Materials. Poly(*N*-vinylcarbazole) (PVK, $M_n \sim 35\,000$, polydispersity ~ 2, density = 1.2 g/cm^3) was purchased from Sigma-Aldrich Chemical Co. (St. Louis, MO). Multiwalled carbon nanotubes (CNTs) were purchased from NanoLab Inc. (Newton, MA). The outer diameter, length, specific surface area, and purity of the CNTs were 15 nm, 5−20 μm, 200−400 m^2/g, and 95%, respectively. The density of multiwalled CNTs is about 2.1 g/cm^3 as reported.[45]

Carbon Nanotube Functionalization. To improve compatibility with the PVK matrix film, the surface of CNT was functionalized with linear alkyl chains (Figure 1), following procedures described in the literature (Supporting Information, Figure S1).[46,47] Multiwall carbon nanotubes, instead of single-wall carbon nanotubes, were used because of their stability and ease of surface modification while maintaining their specific electrical properties. The carboxyl-functionalized multiwall CNTs were first prepared *via* ultrasonication in 1:3 (volume ratio) mixture of concentrated nitric acid/sulfuric acid at 50 °C for 6 h. The mixed acid treatment not only introduced a carboxylic group onto the surface of the CNTs but also removed the amorphous carbon and metal catalyst residues.[48−50] Thus, the electrical properties of the CNTs were not affected by the conductive impurities. The acidic form of CNTs was converted into sodium salt by ultrasonication in 5 mM aqueous NaOH solution. The sodium salt form of CNTs was refluxed with tetrabutylammonium hydrogensulfate and 1-bromododecane until the suspension became clear and the esterified CNTs precipitated out of the solution. The black solids were collected and dried in a vacuum oven at 50 °C overnight. The work function of the CNTs increased from −4.3 to −5.1 eV. The increase was due to the reduction in π conjugation of the CNTs and the increase in inward-pointing surface dipoles caused by the presence of surface carboxylic groups.[32] Esterification of the outer carboxylic groups probably would not affect the π conjugation further. Thus the work function of the esterified CNTs should be similar to that of the acid-treated CNTs (−5.1 eV). The surface-functionalized CNTs also exhibited improved dispersity in organic solvents.

Device Fabrication and Characterization. The electrical properties of PVK−CNT composites were evaluated in ITO/PVK−CNT/Al sandwich devices (Figure 1). The ITO-glass substrates were precleaned by ultrasonication for 15 min each in deionized water, acetone, and 2-propanol, in that order. A 50 μL toluene solution of PVK (10 mg/mL), containing 0−5% of CNTs, was spin-coated onto a precleaned ITO substrate at a spinning speed of 2000 rpm and a duration of 60 s, using a G3P-8 spin-coater (Specialty Coating Systems, Inc.). The film was dried under reduced pressure (10^{-5} Torr) at room temperature overnight. The thickness of the resultant PVK−CNT composite film is around 200 nm, as measured by a step-profiler. Finally, Al was thermally evaporated onto the film surface at 10^{-7} Torr through a shadow mask to form 0.4 × 0.4, 0.2 × 0.2, and 0.15 × 0.15 mm^2 top electrodes with thickness of about 300 nm, using a Leybold UHV Univex 350 thermal evaporation system. Devices with thermally evaporated Cu and Au top electrodes were fabricated similarly.

The as-fabricated devices were characterized under ambient conditions on a probe station (Probing Solutions Inc.), using a Hewlett-Packard 4155B semiconductor parameter analyzer with an Agilent 16440A SMU/pulse generator. The ITO/PVK−CNT/Cu device was characterized at different temperatures on a Cascade Microchamber probe station, with a Keithley 4200 semiconductor parameter analyzer and a Temptronic temperature controlling system. The chemical states of the composite films in the two bistable conductivity states were also analyzed by X-ray photoelectron spectroscopy (XPS). XPS measurements were carried out on a Kratos AXIS HSi spectrometer (Manchester, UK). PVK−CNT composite films for XPS measurements were formed by casting a drop of the toluene solution of PVK−CNT composite onto TEM copper grids, followed by drying under reduced pressure. A removable mercury drop was then introduced on top of the composite film to form the Cu/PVK−CNT/Hg sandwich structure. A voltage of −4 V was applied to the Hg droplet, with the Cu grid as the bottom electrode, using a Keithley 238 current source unit. XPS spectra of the composite films were recorded after removing the Hg droplet electrode. UV−visible absorption spectra corresponding to the two bistable conductivity states of the composite film were obtained similarly with a removable Hg top electrode in the ITO/PVK−CNT/Hg structure, on a Shimadzu UV-3101 PC UV−vis−NIR scanning spectrophotometer.

Supporting Information Available: Procedures for surface functionalization of carbon nanotubes and calculation of effective distance between neighboring carbon nanotubes in the PVK matrices with different CNT loadings. Measurements of switching time in Al/PVK−CNT/ITO bistable devices. This material is available free of charge *via* the Internet at http://pubs.acs.org.

REFERENCES AND NOTES

1. Baughman, R. H.; Zakhidov, A. A.; de Heer, W. A. Carbon Nanotubes: The Route toward Applications. *Science* **2002**, *297*, 787–792.
2. Wang, C.; Guo, Z. X.; Fu, S.; Wu, W.; Zhu, D. Polymers Containing Fullerene or Carbon Nanotube Structures. *Prog. Polym. Sci.* **2004**, *29*, 1079–1141.
3. Huang, J. W.; Bai, S. J. Light Emitting Diodes of Fully Conjugated Heterocyclic Aromatic Rigid-Rod Polymer Doped with Multi-Wall Carbon Nanotubes. *Nanotechnology* **2005**, *16*, 1406–1410.
4. Smith, R. C.; Careya, J. D.; Murphy, R. J.; Blau, W. J.; Coleman, J. N.; Silva, S. R. P. Charge Transport Effects in Field Emission from Carbon Nanotube−Polymer Composites. *Appl. Phys. Lett.* **2005**, *87*, 263105.
5. Xu, Z. H.; Wu, Y.; Hua, B.; Ivanov, I. N.; Geohegan, D. B. Carbon Nanotube Effects on Electroluminescence and Photovoltaic Response in Conjugated Polymers. *Appl. Phys. Lett.* **2005**, *87*, 263118.
6. Ago, H.; Petritsch, K.; Shaffer, M. S. P.; Windle, A. H.; Friend, R. H. Composites of Carbon Nanotubes and Conjugated Polymers for Photovoltaic Devices. *Adv. Mater.* **1999**, *15*, 1281–1285.
7. Kymakis, E.; Amaratunga, G. A. J. Single-Wall Carbon Nanotube/Conjugated Polymer Photovoltaic Devices. *Appl. Phys. Lett.* **2002**, *80*, 112–114.
8. Klinke, C.; Chen, J.; Afzali, A.; Avouris, P. Charge Transfer Induced Polarity Switching in Carbon Nanotube Transistors. *Nano Lett.* **2005**, *5*, 555–558.
9. Valentini, L.; Kenny, J. M. Novel Approaches to Developing Carbon Nanotube Based Polymer Composites: Fundamental Studies and Nanotech Applications. *Polymer* **2005**, *46*, 6715–6718.
10. Star, A.; Lu, Y.; Bradley, K.; Grüner, G. Nanotube Optoelectronic Memory Devices. *Nano Lett.* **2004**, *4*, 1587–1591.
11. Marsman, A. W.; Hart, C. M.; Gelinck, G. H.; Geuns, T. C. T.; de Leeuw, D. M. Doped Polyaniline Polymer Fuses: Electrically Programmable Read-Only-Memory Elements. *J. Mater. Res.* **2004**, *19*, 2057–2060.
12. Pradhan, B.; Batabyal, S. K.; Pal, A. J. Electrical Bistability and Memory Phenomenon in Carbon Nanotube-Conjugated Polymer Matrixes. *J. Phys. Chem. B* **2006**, *110*, 8274–8277.
13. Tang, W.; Shi, H. Z.; Xu, G.; Ong, B. S.; Popovic, Z. D.; Deng, J. C.; Zhao, J.; Rao, G. H. Memory Effect and Negative Differential Resistance by Electrode-Induced Two-Dimensional Single-Electron Tunneling in Molecular and Organic Electronic Devices. *Adv. Mater.* **2005**, *17*, 2307–2311.
14. Kondo, T.; Lee, S. M.; Malicki, M.; Domercq, B.; Marder, S. R.; Kippelen, B. A Nonvolatile Organic Memory Device Using ITO Surfaces Modified by Ag-Nanodots. *Adv. Funct. Mater.* **2008**, *18*, 1112–1118.
15. Forrest, S. R. The Path to Ubiquitous and Low-Cost Organic Electronic Appliances on Plastic. *Nature* **2004**, *428*, 911–918.
16. Reichmanis, E.; Katz, H.; Kloc, C.; Maliakal, A. Plastic Electronic Devices: From Materials Design to Device Applications. *Bell Lab Tech. J.* **2005**, *10*, 87–105.
17. Raymo, F. M. Digital Processing and Communication with Molecular Switches. *Adv. Mater.* **2002**, *14*, 401–414.
18. Taylor, D. M.; Mills, C. A. Memory Effect in the Current−Voltage Characteristic of a Low-Band Gap Conjugated Polymer. *J. Appl. Phys.* **2001**, *90*, 306–309.
19. Möller, S.; Forrest, S. R.; Perlov, C.; Jackson, W.; Taussig, C. Electrochromic Conductive Polymer Fuses for Hybrid Organic/Inorganic Semiconductor Memories. *J. Appl. Phys.* **2003**, *94*, 7811–7819.
20. Vorotyntsev, M. A.; Skompska, M.; Pousson, E.; Goux, J.; Moise, C. Memory Effects in Functionalized Conducting Polymer Films: Titanocene Derivatized Polypyrrole in Contact with THF Solutions. *J. Electroanal. Chem.* **2003**, *552*, 307–317.
21. Bandyopadhyay, A.; Pal, A. J. Tuning of Organic Reversible Switching *via* Self-Assembly Supermolecular Structures. *Adv. Mater.* **2003**, *15*, 1949–1952.
22. Wang, H. P.; Pigeon, S.; Izquierdo, R.; Martel, R. Electrical Bistability by Self-Assembled Gold Nanoparticles in Organic Diodes. *Appl. Phys. Lett.* **2006**, *89*, 183502.
23. Kanwal, A.; Chhowalla, M. Stable, Three Layered Organic Memory Devices from C60 Molecules and Insulating Polymers. *Appl. Phys. Lett.* **2006**, *89*, 203103.
24. Bozano, L. D.; Kean, B. W.; Beinhoff, M.; Carter, K. R.; Rice, P. M.; Scott, J. C. Organic Materials and Thin-Film Structures for Cross-Point Memory Cells Based on Trapping in Metallic Nanoparticles. *Adv. Funct. Mater.* **2005**, *15*, 1933–1939.
25. Ling, Q. D.; Liaw, D. J.; Zhu, C. X.; Chan, D. S. H.; Kang, E. T.; Neoh, K. G. Polymer Electronic Memories: Materials, Devices and Mechanisms. *Prog. Polym. Sci.* **2008**, *33*, 917–978.
26. Chang, T. E.; Kisliuk, A.; Rhodes, S. M.; Brittain, W. J.; Sokolov, A. P. Conductivity and Mechanical Properties of Well-Dispersed Single-Wall Carbon Nanotube/Polystyrene Composite. *Polymer* **2006**, *47*, 7740–7746.
27. Hiroshiba, N.; Tanigaki, K.; Kumashiro, R.; Ohashi, H.; Wakahara, T.; Akasaka, T. C_{60} Field Effect Transistor With Electrodes Modified By La@C82. *Chem. Phys. Lett.* **2004**, *400*, 235–238.
28. Weast, R. C.; Astle, M. J. *CRC Handbook of Chemistry and Physics*, 63rd ed.; CRC Press Inc.: Boca Raton, FL, 1982; p E-78.
29. Kawamura, Y.; Yanagida, S.; Forrest, S. R. Energy Transfer in Polymer Electrophosphorescent Light Emitting Devices with Single and Multiple Doped Luminescent Layers. *J. Appl. Phys.* **2002**, *92*, 87–93.
30. van Dijken, A.; Bastiaansen, J. J. A. M.; Kiggen, N. M. M.; Langereld, B. M. W.; Rothe, C.; Monkman, A.; Bach, I.; Stossel, P.; Brunner, K. Carbazole Compounds as Host Materials for Triplet Emitters in Organic Light-Emitting Diodes: Polymer Hosts for High-Efficiency Light-Emitting Diodes. *J. Am. Chem. Soc.* **2004**, *126*, 7718–7727.
31. Lim, S. L.; Ling, Q. D.; Teo, E. Y. H.; Zhu, C. X.; Chan, D. S. H.; Kang, E. T.; Neoh, K. G. Conformation-Induced Electrical Bistability in Non-conjugated Polymers with Pendant Carbazole Moieties. *Chem. Mater.* **2007**, *19*, 5148–5157.

32. Ago, H.; Kugler, T.; Cacialli, F.; Salaneck, W. R.; Shaffer, M. S. P.; Windle, A. H.; Friend, R. H. Work Functions and Surface Functional Groups of Multiwall Carbon Nanotubes. *J. Phys. Chem. B* **1999**, *103*, 8116–8121.
33. Gohel, A.; Chin, K. C.; Zhu, Y. W.; Chow, C. H.; Wee, A. T. S. Field Emission Properties of N_2 and Ar Plasma-Treated Multi-Wall Carbon Nanotubes. *Carbon* **2005**, *43*, 2530–2535.
34. Verbakel, F.; Meskers, S. C. J.; Janssen, R. A. J.; Gomes, H. L.; Cölle, M.; Büchel, M.; de Leeuw, D. M. Reproducible Resistive Switching in Nonvolatile Organic Memories. *Appl. Phys. Lett.* **2007**, *91*, 192103.
35. Cölle, M.; Büchel, M.; de Leeuw, D. M. Switching and Filamentary Conduction in Non-volatile Organic Memories. *Org. Electron.* **2006**, *7*, 305–312.
36. Jakobsson, F. L. E.; Crispin, X.; Cölle, M.; Büchel, M.; de Leeuw, D. M.; Berggren, M. On the Switching Mechanism in Rose Bengal-Based Memory Devices. *Org. Electron.* **2007**, *8*, 559–565.
37. Gomes, H. L.; Benvenho, A. R. V.; de Leeuw, D. M.; Cölle, M.; Stallinga, P.; Verbakel, F.; Taylor, D. M. Switching in Polymeric Resistance Random-Access Memories (RRAMS). *Org. Electron.* **2008**, *9*, 119–128.
38. Joo, W. J.; Choi, T. L.; Lee, J.; Lee, S. K.; Jung, M. S.; Kim, N.; Kim, J. M. Metal Filament Growth in Electrically Conductive Polymers for Nonvolatile Memory Application. *J. Phys. Chem. B* **2006**, *110*, 23812–23816.
39. Grazulevivius, J. V.; Strohrirgl, P.; Pielichowski, J.; Pielichowski, K. Carbazole-Containing Polymers: Synthesis, Properties and Applications. *Prog. Polym. Sci.* **2003**, *28*, 1297–1353.
40. Zhang, Y. D.; Wada, T.; Sasabe, H. Carbazole Photorefractive Materials. *J. Mater. Chem.* **1998**, *8*, 809–828.
41. Choi, J. S.; Kim, J. H.; Kim, S. H.; Suh, D. H. Nonvolatile Memory Device Based On the Switching by the All-Organic Charge Transfer Complex. *Appl. Phys. Lett.* **2006**, *89*, 152111.
42. Sze, S. M. *Physics of Semiconductor Devices*, 2nd ed.; Wiley: New York, 1981; p 227.
43. Murgatroyd, P. N. Theory of Space-Charge-Limited Current Enhanced by Frenkel Effect. *J. Phys. D* **1970**, *3*, 151–156.
44. Johansson, Å.; Stafström, S. Modeling of the Dynamics of Charge Separation in an Excited Poly(phenylene vinylene)/C60 System. *Phys. Rev. B* **2003**, *68*, 035206.
45. Lu, Q.; Keskar, G.; Ciocan, R.; Rao, R.; Mathur, R. B.; Rao, A. M.; Larcom, L. L. Determination of Carbon Nanotube Density by Gradient Sedimentation. *J. Phys. Chem. B* **2006**, *110*, 24371–24376.
46. Qin, Y.; Shi, J.; Wu, W.; Li, X.; Guo, Z.-X.; Zhu, D. Concise Route to Functionalized Carbon Nanotubes. *J. Phys. Chem. B* **2003**, *107*, 12899–12901.
47. Liu, G.; Ling, Q. D.; Chang, F. C.; Liaw, D. J.; Zhu, C. X.; Chan, D. S. H.; Kang, E. T.; Neoh, K. G. Bistable Electrical Switching and Write-Once Read-Many-Times Memory Effect in a Donor−Acceptor Containing Polyfluorene Derivative and Its Carbon Nanotube Composites. *J. Appl. Phys.* **2007**, *102*, 024502.
48. Liu, J.; Rinzler, A. G.; Dai, H.; Hafner, J. H.; Bradley, R. K.; Boul, P. J.; Lu, A.; Iverson, T.; Shelimov, K.; Huffman, C. B.; et al. Fullerene Pipes. *Science* **1998**, *280*, 1253–1256.
49. Li, S.; Qin, Y.; Shi, J.; Guo, Z. X.; Li, Y.; Zhu, D. Electrical Properties of Soluble Carbon Nanotube/Polymer Composite Films. *Chem. Mater.* **2005**, *17*, 130–135.
50. Aguirre, C. M.; Auvray, S.; Pigeon, S.; Izquierdo, R.; Desjardins, P.; Martel, R. Carbon Nanotube Sheets as Electrodes in Organic Light-Emitting Diodes. *Appl. Phys. Lett.* **2006**, *88*, 183104.